Diamond Sampling for Approximate Maximum All-pairs Dot-product (MAD) Search

Grey Ballard, Tamara G. Kolda, and Ali Pinar
Data Sciences & Cyber Analytics Department
Sandia National Laboratories
Livermore, CA
gmballa@sandia.gov, tgkolda@sandia.gov, apinar@sandia.gov

C. Seshadhri
Department of Computer Science
University of California
Santa Cruz, CA
scomandu@ucsc.edu

Abstract—Given two sets of vectors, $A = \{\vec{a_1}, \ldots, \vec{a_m}\}$ and $B = \{\vec{b_1}, \ldots, \vec{b_n}\}$, our problem is to find the top-t dot products, i.e., the largest $|\vec{a_i} \cdot \vec{b_j}|$ among all possible pairs. This is a fundamental mathematical problem that appears in numerous data applications involving similarity search, link prediction, and collaborative filtering. We propose a sampling-based approach that avoids direct computation of all mn dot products. We select diamonds (i.e., four-cycles) from the weighted tripartite representation of A and B. The probability of selecting a diamond corresponding to pair (i, j) is proportional to $(\vec{a_i} \cdot \vec{b_j})^2$, amplifying the focus on the largest-magnitude entries. Experimental results indicate that diamond sampling is orders of magnitude faster than direct computation and requires far fewer samples than any competing approach. We also apply diamond sampling to the special case of maximum inner product search, and get significantly better results than the state-of-the-art hashing methods.

I. Introduction

Finding similar items is a fundamental problem that underlies numerous problems in data analysis. Link prediction in a graph can be cast as finding similar nodes in the graph [1], [2]; customers are recommended similar products [3]; text analysis often involves finding similar texts [4], [5]; data cleaning requires removal of entries that are essentially identical [6]. In these settings, entities are represented as vectors in high-dimensional feature space, i.e., $\vec{v} \in \mathbb{R}^d$, for some large d. Many notions of similarity involve dot products, so a measure of distance between $\vec{v}$ and $\vec{w}$ is $\vec{v} \cdot \vec{w}$. This subsumes cosine similarity, common-neighbors, database join operations [7], frequent itemset mining, data cleaning [6], etc. Motivated by these applications, we study the Maximum All-pairs Dot-product (MAD) problem.

DEFN. 1 (t-MAD: MAX ALL-PAIRS DOT-PRODUCT). Given two sets of d-dimensional vectors $A = \{\vec{a_1}, \ldots, \vec{a_m}\}$ and $B = \{\vec{b_1}, \ldots, \vec{b_n}\}$: find the index pair (i, j) that maximizes $|\vec{a_i} \cdot \vec{b_j}|$. More generally, given additional parameter t, find the t index pairs $\{(i_1, j_1), \ldots, (i_t, j_t)\}$ corresponding to the t largest dot products.

It is convenient to think of A and B as matrices ($A \in \mathbb{R}^{d \times m}$ and $B \in \mathbb{R}^{d \times n}$), where the columns are the corresponding vectors. The MAD problem is exactly finding the largest entries in the product $C = A^T B \in \mathbb{R}^{m \times n}$.
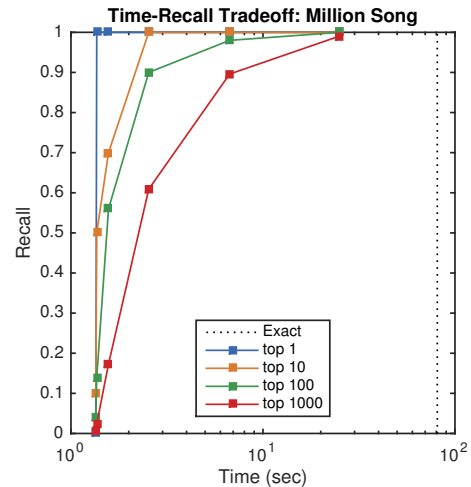

Fig. 1: Million song dataset [10], [11], [12]: Dataset with 350K songs, and 48M user-song entries. Diamond sampling finds top 100 correlated songs within 7 seconds, while exhaustive search takes around 80 seconds.

The MAD formulation subsumes many existing problems in the literature. For the special case where A is a single column (equivalently, $m = 1$), this is the exactly the MIPS (Maximum Inner Product Search) problem [8], [9]. Here, we maximize the dot product with $\vec{a}$ among all columns of B. When $A = B$ is the adjacency matrix of a graph, this is equivalent to finding pairs of nodes with the most common neighbors, a fundamental link prediction operation.

A. Difficulties with previous art

The most obvious approach is to simply compute $A^T B$ exhaustively. There is a rich history on algorithms for dense and sparse matrix multiplication [13], [14], with implementations in libraries like Intel MKL's BLAS [15] and CSparse [16]. However, existing algorithms become prohibitive as the sizes of A and B grow, even if they are sparse.

There is also much literature in approximate matrix multiplication, which quickly computes an approximate product $\tilde{C} \approx A^T B$. Drineas, Kannan, and Mahoney [17], [18] introduced an approach based on sampling rows of A and B to minimize Frobenius norm of the error. Much study has been

done on various sampling strategies [19], [20], [21], [22], [23], [24]. These methods are also not suited for MAD, since we only care for a few entries (at most, say, 1000) despite the matrix having dimensions in the millions.

An alternate, popular approach for high-dimensional nearest neighbor search is some form of dimension reduction, the most famous approach being Indyk and Motwani's Locality Sensitive Hashing (LSH) [25], [26], [27]. Recent results by Shrivastava and Li extend LSH methods for the MIPS problem [9]. These approaches usually involve randomly hashing the vectors into a few "buckets", and then searching for vector pairs that share many common buckets. For high-dimensional data, the maximum dot product is often small in comparison to the vector norms, so the similarities are quite small. This means that many hashes are required to find the nearest neighbors, leading to a storage blowup (typically, two orders of magnitude more than the data). This can be quite prohibitive even for small data sets.

B. The sampling approach

We take a different route, and apply *index sampling* methods. The idea is to sample pair (i, j) proportional to some function of the dot product $\vec{a_i} \cdot \vec{b_j}$. With enough samples, we hope to find the large entries of $C = A^T B$. The earliest application of this idea is by Cohen and Lewis, who constructed a sampling algorithm for the MIPS problem [28], [8]. Their approach samples pairs (i, j) proportional to $\vec{a_i} \cdot \vec{b_j}$ [28], [8]. Campagna and Pagh give sampling approaches for a variety of distance measures [29].

We stress that no previous result (either sampling based, LSH based, or otherwise) applies directly to the MAD problem.

C. Our Contributions

Diamond sampling: Our main contribution is *diamond sampling*, a new randomized approach to the MAD problem. This is inspired by recent work by Jha et al for 4-vertex motif detection in large graphs [30]. Their idea is to sample 3-paths in graphs to estimate counts of 4-vertex motifs. We generalize that idea to the matrix product setting, to design a sampling procedure for the MAD problem. Diamond sampling is able to sample pairs (i, j) proportional to $(\vec{a_i} \cdot \vec{b_j})^2$. The square term is a critical improvement over Cohen and Lewis; it allows for faster convergence to the top entries of $C = A^T B$.

Theoretical analysis: We give a theoretical analysis of diamond sampling, and prove concentration bounds on its behavior. Our analysis shows the eventual convergence of the sampling to squared entries, with no assumption whatsoever. Previous sampling work required nonnegativity assumption, or assumed structural correlations among positive entries [28], [8]. We give strong storage bounds on diamond sampling, and show that it requires very little overhead.

Empirical validation: We apply diamond sampling on six real-world datasets and show that is extremely efficient. Diamond sampling is orders of magnitude faster than exact computation and requires far fewer samples compared to other matrix sampling approaches. Fig. 1 shows the results of diamond sampling on a song dataset with 48M user-song entries. We consider $A = B$ to be the matrix where songs are columns and attempt to find the top correlated songs. We can get the top 100 pairs in an order of magnitude less time than exhaustive computation.

We consider numerous applications in product recommendation and link prediction, and consistently get to top 10-100 dot products, with a speedup of 10-100X over exact computation. Furthermore, the number of samples required is much smaller than the Cohen-Lewis approach [8].

Application to MIPS: Given recent interest in the MIPS problem, we also apply diamond sampling to a MIPS problem, as used in [9]. We focus on the MovieLens dataset [31], a collaborative filtering application. We get significantly better precision-recall curves with a maximum precision of 90-100% as opposed to 30-65% with asymmetric LSH methods. Our running time is a fraction of a second per query. Our diamond sampling requires minimal storage overhead and much less than LSH methods, which require large amounts of memory, easily running into hundred times the dataset size (requiring a large-memory machine).

II. PRELIMINARIES AND NOTATION

We use the standard notation that $[n] = \{1, \ldots, n\}$. For $x \in \mathbb{R}$, the function $\text{sgn}(x) = 1$ if $x \geq 0$ and -1 otherwise; i.e., $x = \text{sgn}(x)|x|$. Let $\vec{v} \in \mathbb{R}^n$ denote a vector and $M = (m_{ij}) \in \mathbb{R}^{m \times n}$ be a matrix. We denote the vector and matrix p-norms as follows:

$$\|\vec{v}\|_p^p = \sum_{i=1}^{n} |v_i|^p \quad \text{and} \quad \|M\|_p^p = \sum_{i=1}^{m} \sum_{j=1}^{n} |m_{ij}|^p. \quad (1)$$

Note that the matrix p-norms are entrywise rather than the induced norms. We let $\text{nnz}(M)$ denote the number of nonzeros in M; if M is dense, then we suppose without loss of generality that $\text{nnz}(M) = mn$.

We assume throughout that $A \in \mathbb{R}^{d \times m}$ and $B \in \mathbb{R}^{d \times n}$. We use $k, k' \in [d]$ to index rows of A and B. The kth rows of A and B (transposed to column vectors) are denoted by a_{k*} and b_{k*} respectively. We use $i, i' \in [m]$ to index columns of A, whose ith column is denoted by $\vec{a_i}$ or a_{*i}. We use $j, j' \in [n]$ to index columns of B, whose jth column is denoted by $\vec{b_j}$ or b_{*j}. Since, by definition, $C = A^T B$, we have

$$c_{ij} = \vec{a_i} \cdot \vec{b_j} = \sum_{k} a_{ki} b_{kj} \quad \text{for all} \quad i \in [m], \ j \in [n].$$

If A and B are binary, i.e., unweighted adjacency matrices, then we can consider them as representing a tripartite graph on $m + d + n$ nodes; see Fig. 2. From this interpretation, we define the neighbor sets,

$$\mathcal{N}_i^A = \{ k \in [d] \mid a_{ki} = 1 \}, \quad \mathcal{N}_k^A = \{ i \in [m] \mid a_{ki} = 1 \},$$
$$\mathcal{N}_j^B = \{ k \in [d] \mid b_{kj} = 1 \}, \quad \mathcal{N}_k^B = \{ j \in [n] \mid b_{kj} = 1 \}.$$

Correspondingly, we can define degrees of the nodes, i.e.,

$$\deg_i^A = |\mathcal{N}_i^A| = \|a_{*i}\|_1, \deg_k^A = |\mathcal{N}_k^A| = \|a_{k*}\|_1,$$
$$\deg_j^B = |\mathcal{N}_j^B| = \|b_{*j}\|_1, \deg_k^B = |\mathcal{N}_k^B| = \|b_{k*}\|_1.$$

Random selection is uniform, i.e., equal probability for all elements of a discrete set, unless stated otherwise.

III. DIAMOND SAMPLING

Complexity of diamond sampling depends on the two input matrices. We start our discussion with the special case of binary matrices A and B. We follow with the general case and then discuss other special cases such as nonnegative inputs and computing the maximum in $A^T A$, i.e., $B = A$.

A. Binary inputs

To motivate our procedure, we start with the case where A and B are binary matrices. We can represent this as a tripartite graph where the m columns of A, indexed by i, correspond to nodes on the left; the n columns of B, indexed by j, correspond to nodes on the right; and the d common rows of A and B, indexed by k or k', correspond to nodes in the center. Edge (i, k) exists iff $a_{ki} = 1$; likewise, edge (k, j) exists iff $b_{kj} = 1$. Therefore, c_{ij} is simply the number of common neighbors of i and j:

$$c_{ij} = \vec{a_i} \cdot \vec{b_j} = |\{\, k \mid k \in \mathcal{N}_i^A \cap \mathcal{N}_j^B \,\}|.$$

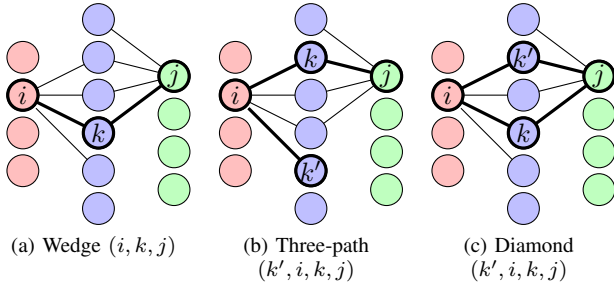(a) Wedge (i, k, j) (b) Three-path (k', i, k, j) (c) Diamond (k', i, k, j)

Fig. 2: Illustration of tripartite graph. For simplicity, we show only those edges incident nodes i or j.

If node k has an A-neighbor i and a B-neighbor j, then we call (i, k, j) a "wedge." The existence of such a wedge implies that $c_{ij} \geq 1$. In fact, there are exactly c_{ij} distinct wedges connecting pair (i, j); see Fig. 2a. The probability of selecting a random wedge with endpoints (i, j) can be shown to be proportional to c_{ij} [28], [8].

In diamond sampling, our goal is find a "diamond" (k', i, k, j) formed by *two* intersecting wedges, i.e., (i, k, j) and (i, k', j); see Fig. 2c. Note that any pair (i, j) participates in c_{ij}^2 diamonds (note that we are not requiring k and k' to be different). Hence, the probability of selecting a random diamond of the form (k', i, k, j) is proportional to c_{ij}^2.

Sampling random diamonds will expedite identifying the largest dot products as compared to sampling random wedges; however, sampling random diamonds is more complex. Thankfully, we can adapt the arguments of Jha et al. [30] for this

purpose. Here, the goal is to find a random three-path of the form (k', i, k, j). If it closes to form a four-cycle, then it is a random diamond. Moreover, these samples will be uncorrelated. That is, given a set of random 3-paths, those that complete to a diamond will form a uniform sample of the diamonds. See Fig. 2c for a three-path that closes to form a diamond and Fig. 2b for one that does not.

Finding a random three-path of the form (k', i, k, j) is a multi-step procedure, shown in Algorithm 1 and illustrated in Fig. 3. In Line 2, we weight each edge (i, k) according to the number of three paths it is the center of, i.e., $\deg_i^A \deg_k^B$ (again we do not require $k \neq k'$), and store the weights in a matrix W. Observe that W has the same sparsity pattern as A. In Line 6, we select a random edge (i, k) proportional to its weight (see Fig. 3a). To complete the three-path, we select a random neighbor of k in B, labeled j in Line 7 (see Fig. 3b) and a random neighbor of i in A, labeled k' in Line 8 (see Fig. 3c). This yields a uniform random three-path. If edge (k', j) exists, i.e., $b_{k'j} = 1$, then the three-path is a diamond and so we increment the counter x_{ij} in Line 9; obviously, $\mathrm{nnz}(X) \leq s$.

Algorithm 1 Diamond sampling with binary inputs

Given matrices $A \in \{0, 1\}^{m \times d}$ and $B \in \{0, 1\}^{n \times d}$.
Let s be the number of samples.

1: **for** $(k, i) \in [d] \otimes [m]$ **do**
2:     $w_{ki} \leftarrow a_{ki} \deg_i^A \deg_k^B$
3: **end for**
4: $X \leftarrow$ all-zero matrix of size $m \times n$
5: **for** $\ell = 1, \ldots, s$ **do**
6:     Sample (k, i) with probability $w_{ki}/\|W\|_1$
7:     Sample j from $\mathcal{N}_k^B$
8:     Sample k' from $\mathcal{N}_i^A$
9:     $x_{ij} \leftarrow x_{ij} + b_{k'j}$
10: **end for**
11: Postprocessing (see Algorithm 2)

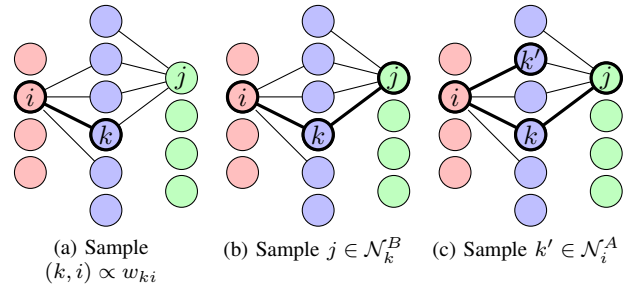(a) Sample $(k, i) \propto w_{ki}$ (b) Sample $j \in \mathcal{N}_k^B$ (c) Sample $k' \in \mathcal{N}_i^A$

Fig. 3: Illustration of diamond sampling in Algorithm 1. For simplicity, we show only those edges incident nodes i or j.

The largest values in X correspond to the (likely) largest dot products, but we do some further postprocessing to obtain the final answer, as shown in Algorithm 2. We are seeking the top-t dot products. We have a budget of $t' \geq t$ dot products,

where we assume $t' \ll mn$. We let Ω_s denote the indices of all the nonzeros in X and $\Omega_{t'}$ denote the top-t' entries in X; this requires a sort in Line 1 of at most s items (and generally many fewer, depending on the proportion of three-paths that close into diamonds). We compute the t' dot products in Lines 3 to 5 at a cost of $O(t'd)$. Finally, we let Ω_t denote the top-t dot products from $\Omega_{t'}$ in Line 6, requiring a sort of t' items.

Algorithm 2 Postprocessing

Given $\Omega_s = \{ (i,j) \mid x_{ij} > 0 \}$. Let t be the number of top dot products, and $t' \geq t$ be the budget of dot products.

1: Extract top-t' entries of X, i.e., $|\Omega_{t'}| \leq t'$ and
   $\Omega_{t'} \leftarrow \{ (i,j) \in \Omega_s \mid x_{ij} \geq x_{i'j'} \forall (i',j') \in \Omega_s \setminus \Omega_{t'} \}$
2: $C \leftarrow$ all-zero matrix of size $m \times n$
3: **for** $(i,j) \in \Omega_{t'}$ **do**
4: $\quad c_{ij} \leftarrow a_i^T b_j$
5: **end for**
6: Extract top-t entries of C, i.e., $|\Omega_t| \leq t$ and
   $\Omega_t \leftarrow \{ (i,j) \in \Omega_{t'} \mid c_{ij} \geq c_{i'j'} \forall (i',j') \in \Omega_{t'} \setminus \Omega_t \}$

B. General inputs

We present the binary version as general motivation, but our implementation and analysis are based on the diamond sampling algorithm for general real-valued A and B in Algorithm 3. In this case, we define the matrix of weights $W \in \mathbb{R}^{d \times n}$ such that

$$w_{ki} = |a_{ki}| \, \|a_{*i}\|_1 \|b_{k*}\|_1 \quad \text{for all} \quad k \in [d], \ i \in [m].$$

The weight w_{ki} correspond to the weight of all three paths with edge (i,k) at its center. This is computed in Line 2. The sampling in Line 6 has the same complexity as in the binary case, but the sampling in Lines 7 and 8 now has a nonuniform distribution and so has higher complexity than in the binary case. The postprocessing is unchanged.

Algorithm 3 Diamond sampling with general inputs

Given matrices $A \in \mathbb{R}^{m \times d}$ and $B \in \mathbb{R}^{n \times d}$.
Let s be the number of samples.

1: **for all** $a_{ki} \neq 0$ **do**
2: $\quad w_{ki} \leftarrow |a_{ki}| \, \|a_{*i}\|_1 \|b_{k*}\|_1$
3: **end for**
4: $X \leftarrow$ all-zero matrix of size $m \times n$
5: **for** $\ell = 1, \ldots, s$ **do**
6: $\quad$ Sample (k,i) with probability $w_{ki}/\|W\|_1$
7: $\quad$ Sample j with probability $|b_{kj}|/\|b_{k*}\|_1$
8: $\quad$ Sample k' with probability $|a_{k'i}|/\|a_{*i}\|_1$
9: $\quad x_{ij} \leftarrow x_{ij} + \text{sgn}(a_{ki}b_{kj}a_{k'i}) \, b_{k'j}$
10: **end for**
11: Postprocessing (see Algorithm 2)

---

1) Nonnegative inputs: If A and B are nonnegative, the only change is that the sign computations can be ignored in computing the sample increment in Line 9 in Algorithm 3. This avoids potentially expensive random memory accesses.

2) Equal inputs (Gram matrix): If $B = A$, then $C = A^T A$ is symmetric. The matrix X is not symmetric, although $\mathbb{E}[X]$ is. Hence, we modify X before by inserting the following step before the postprocessing in Line 11 in Algorithm 3:

$$X \leftarrow (X + X^T)/2. \tag{2}$$

Now X is symmetric, and the forthcoming analysis is unaffected.

3) Equal symmetric inputs (squared matrix): If $B = A$ and A is symmetric, then $C = A^2$ and we can replace Line 9 in Algorithm 3 with the following two lines:

$$x_{ij} \leftarrow x_{ij} + \text{sgn}(a_{ki}b_{kj}a_{k'i}) \, b_{k'j}/2,$$
$$x_{kk'} \leftarrow x_{kk'} + \text{sgn}(a_{ki}b_{kj}a_{k'i}) \, b_{k'j}/2.$$

This exploits the fact that we can swap the role of k and i in the initial edge sample. Again, X may not be symmetric, so we insert (2) before the postprocessing in Line 11.

C. Complexity and space

Let $\alpha = \text{nnz}(A)$ and $\beta = \text{nnz}(B)$. In the dense case, $\alpha = md$ and $\beta = nd$. The total work is

$$O(\alpha + \beta + s \log(s\alpha\beta)).$$

The total storage (not counting the inputs A and B) is

$$2\,\text{storage}(A) + \text{storage}(B) + 5s + 3t' + 3t.$$

We give detailed arguments below and in the implementation discussion in Section V.

Preprocessing. For the sampling in Lines 7 and 8, we precompute cumulative, normalized column sums for B and the same for rows of A, requiring storage of $\text{storage}(A) + \text{storage}(B)$ and computation of $O(\alpha + \beta)$. The matrix W has the same nonzero pattern as A, so the cost to store it is equal to $\text{storage}(A)$ and to compute it is $O(\alpha)$.

Sampling. For a straightforward implementation, the cost per sample in Line 6 is $O(\log(\alpha))$. For Line 7, the cost per sample is $O(\log(\beta/d))$; here, we have used the approximation $\text{nnz}(b_{k*}) \approx \beta/d$. A similar analysis applied for A and Line 8. So, the cost per sample is $O(\log(\alpha) + \log(\beta/d) + \log(\alpha/m))$. Without loss of generality, we assume that we need to store the three-paths and the summand in Line 9 for a total storage of $5s$.

Postprocessing. Conservatively, we require $3t'$ storage for the $(i, j, x_{ij}$ or $c_{ij})$ triples in $\Omega_{t'}$ and $3t$ storage for the (i, j, c_{ij}) triples in Ω_t. The sorting requires at most $O(s \log s)$ time, and usually much less since $\text{nnz}(X)$ may be much less than s due to only some three-paths forming diamonds and concentration, i.e., picking the same (i, j) pair multiple times.

IV. ANALYSIS OF DIAMOND SAMPLING

This section provides a theoretical analysis of diamond sampling. We first prove that the expected value of x_{ij} is $c_{ij}^2/\|W\|_1$, and then we prove error bounds on our estimate as a function of the number of samples. Unless stated otherwise, our analysis applies to the general version of the diamond-sampling algorithm (Algorithm 3).

A. Expectation

For a single instance of Lines 6 to 8 of Algorithm 3, we define the event

$$\mathcal{E}_{k'ikj} = \text{choosing three-path } (k', i, k, j).$$

LEMMA 1. $\Pr(\mathcal{E}_{k'ikj}) = |a_{ki}b_{kj}a_{k'i}|/\|W\|_1.$

Proof: The probability of choosing three-path (k', i, k, j) is (by independence of these choices) the product of the following probabilities: that of choosing the center edge (i, k), then picking j, and then picking k'.

$$\Pr(\mathcal{E}_{k'ijk}) = \Pr(\text{ctr } (i,k)) \cdot \Pr(\text{endpts } j \text{ and } k'|\text{ctr } (i,k))$$
$$= \frac{w_{ki}}{\|W\|_1} \cdot \frac{|b_{kj}|}{\|b_{k*}\|_1} \cdot \frac{|a_{k'i}|}{\|a_{*i}\|_1}$$
$$= \frac{|a_{ki}|\|a_{*i}\|_1\|b_{k*}\|_1}{\|W\|_1} \cdot \frac{|b_{kj}|}{\|b_{k*}\|_1} \cdot \frac{|a_{k'i}|}{\|a_{*i}\|_1}$$
$$= \frac{|a_{ki}b_{kj}a_{k'i}|}{\|W\|_1}.$$

In what follows, we use $X_{i,j,\ell}$ to be the following random variable: if i, j are the respective indices updated in the ℓth iteration, $X_{i,j,\ell} = \text{sgn}(a_{ki}b_{ki}a_{k'i})b_{k'j}$. Otherwise, $X_{i,j,\ell} = 0$. Observe that $x_{ij} = \sum_{\ell=1}^{s} X_{i,j,\ell}$.

LEMMA 2. *For diamond sampling, $\mathbb{E}[x_{ij}/s] = c_{ij}^2/\|W\|_1$.*

Proof: We note that $\mathbb{E}[x_{ij}/s] = \mathbb{E}[\sum_\ell X_{i,j,\ell}]/s = \mathbb{E}[X_{i,j,1}]$. (We use linearity of expectation and the fact that the $X_{i,j,\ell}$ are i.i.d. for fixed i, j and varying ℓ.)

$$\mathbb{E}[X_{i,j,1}] = \sum_k \sum_{k'} \Pr(\mathcal{E}_{k'ikj}) \cdot \text{sgn}(a_{ki}b_{ki}a_{k'j}) b_{k'j}$$
$$= \sum_k \sum_{k'} \frac{|a_{ki}b_{kj}a_{k'i}|}{\|W\|_1} \cdot \text{sgn}(a_{ki}b_{kj}a_{k'i}) b_{k'j}$$
$$= \frac{1}{\|W\|_1} \sum_k \sum_{k'} a_{ki}b_{kj}a_{k'i}b_{k'j}$$
$$= \frac{1}{\|W\|_1} \left(\sum_k a_{ki}b_{kj}\right)\left(\sum_{k'} a_{k'i}b_{k'j}\right)$$
$$= \frac{1}{\|W\|_1} \left(\sum_k a_{ki}b_{kj}\right)^2 = \frac{c_{ij}^2}{\|W\|_1}.$$

B. Concentration bounds

We now provide some concentration bounds when all entries in A and B are nonnegative.

LEMMA 3. *Fix $\varepsilon > 0$ and error probability $\delta \in (0, 1)$. Assume all entries in A and B are nonnegative and at most K. If the number of samples*

$$s \geq 3K\|W\|_1 \log(2/\delta)/(\varepsilon^2 c_{ij}^2),$$

then

$$\Pr[|x_{ij}\|W\|_1/s - c_{ij}^2| > \varepsilon c_{ij}^2|] \leq \delta.$$

Proof: Observe that $X_{i,j,\ell}$ is in the range $[0, K]$. Thus, $Y_{i,j,\ell} = X_{i,j,\ell}/K$ is in $[0, 1]$. Set $y_{ij} = \sum_\ell Y_{i,j,\ell}$. Since y_{ij} is the sum of random variables in $[0, 1]$, we can apply the standard multiplicative Chernoff bound (Theorem 1.1 of [32]). This yields $\Pr[y_{ij} \geq (1+\varepsilon)\mathbb{E}[y_{ij}]] < \exp(-\varepsilon^2\mathbb{E}[y_{ij}]/3)$. By Lemma 2, $\mathbb{E}[y_{ij}] = (s/K)(c_{ij}^2/\|W\|_1)$, which is at least $3\log(2/\delta)/\varepsilon^2$ by choice of s. Hence, $\Pr[y_{ij} \geq (1+\varepsilon)\mathbb{E}[y_{ij}]] < \delta/2$. Note that $y_{ij} = x_{ij}/K$. We multiply the expression inside the $\Pr[\cdot]$ by $K\|W\|_1/s$ to get the event $x_{ij}\|W\|_1/s \geq (1+\varepsilon)c_{ij}^2$.

Using the Chernoff lower tail bound and identical reasoning, we get $\Pr[x_{ij}\|W\|_1/s \leq (1-\varepsilon)c_{ij}^2] \leq \delta/2$. A union bound completes the proof. ∎

The following theorem gives a bound on the number of samples required to distinguish "large" dot products from "small" ones. The constant 4 that appears is mostly out of convenience; it can be replaced with anything > 1 with appropriate modifications to s.

THEOREM 4. *Fix some threshold τ and error probability $\delta \in (0, 1)$. Assume all entries in A and B are nonnegative and at most K. Suppose $s \geq 12K\|W\|_1 \log(2mn/\delta)/\tau^2$. Then with probability at least $1 - \delta$, the following holds for all indices i, j and i', j': if $c_{ij} > \tau$ and $c_{i'j'} < \tau/4$, then $x_{ij} > x_{i'j'}$.*

Proof: First consider some dot product c_{ij} with value at least τ. We can apply Lemma 3 with $\varepsilon = 1/2$ and error probability δ/mn, so with probability at least $1 - \delta/mn$, $x_{ij}\|W\|_1/s \geq c_{ij}^2/2 \geq \tau^2/2$. Now consider dot product $c_{i'j'} < \tau/3$. Define $y_{i'j'}$ and $Y_{i',j',\ell}$ as in the proof of Lemma 3. We can apply the lower tail bound of Theorem 1.1 (third part) of [32]: for any $b > 2e\mathbb{E}[y_{i'j'}]$, $\Pr[y_{i'j'} > b] < 2^{-b}$.

We set $b = s\tau^2/2K\|W\|_1$. From Lemma 2 and the assumption that $c_{i'j'} < \tau/3$ and $\mathbb{E}[y_{i'j'}] = \mathbb{E}[x_{i'j'}]/K = sc_{i'j'}^2/K\|W\|_1 \leq s\tau^2/(16K\|W\|_1) < b/2e$. Plugging in our bound for s, $b \geq (12K\|W\|_1 \log(2mn/\delta)/\tau^2)\cdot\tau^2/(2K\|W\|_1) = 6\log(2mn/\delta)$. Hence, $\Pr[y_{i'j'} > b] < \delta/(2mn)$. Equivalently, $\Pr[x_{i'j'}\|W\|_1/s > \tau^2/2] < \delta/(2mn)$. We take a union bound over all the error probabilities (there are at most mn pairs i, j or i', j').

In conclusion, with probability at least $1-\delta$, for any pair of indices i, j: if $c_{ij} > \tau$, then $x_{ij}\|W\|_1/s \geq \tau^2/2$. If $c_{ij} < \tau/4$, then $x_{ij}\|W\|_1/s < \tau^2/2$. This completes the proof. ∎

To get a useful interpretation of Lemma 3 and Theorem 4, we ignore the parameters ε and δ. Let us also assume that $K = 1$, which is a reasonable assumption for most of our experiments. Basically, to get a reasonable estimate of c_{ij}, we require $\|W\|_1/c_{ij}^2$ samples. If the value of the t-th largest entry in C is τ, we require $\|W\|_1/\tau^2$ samples to find the t-largest entries. For instance, on a graph, if we want to identify pairs of vertices with at least 200 common neighbors, we can set $\tau = 200$, and $\|W\|_1$ will be the number of (non-induced) 3-paths in the graph. The square in the denominator is what makes this approach work. In Table I of Section VI, we show some of the values of $\|W\|_1/\tau^2$ for particular datasets, where τ is the magnitude of the largest entry.

V. IMPLEMENTATION DETAILS

We discuss the implementation details for reproducibility, but we stress that the implementation is not our primary contribution. Nevertheless, careful thought has gone into the process and we show that a clever implementation of the sampling can improve performance by almost $3\times$; see Fig. 4.

A. Sampling from discrete distributions

We consider two alternative schemes for drawing s samples from an arbitrary discrete distribution defined by the vector $\vec{\rho} \in [0,1]^p$ such that $\sum_{k=1}^{p} \rho_k = 1$. The choice of schemes is based on the relative sizes of s and p.

If the size of the distribution, p, is smaller than the number of samples, s, then we use binary search on the cumulative sums of ρ to determine each sample. This requires $O(s \log p)$ comparisons, plus $O(p)$ work for the preprocessing to compute the cumulative sum. We note that using the alias method [33] yields a constant time per search at the same cost for preprocessing and storage (up to a constant). The cumulative sum requires $O(p)$ space, and sampled events are stored as counts in space $O(p)$. Note that both the binary search and sample counter increments involve random (not contiguous) memory access. This returns a count vector $\vec{c}$ of length p such that c_k is the number of occurrences of event k and $\sum c_k = s$.

If, on the other hand, the number of samples, s, is less than the size of the distribution, p, we can avoid the binary search by doing a single sort of the samples, as shown in Algorithm 4. This is essentially a variation on merge sort, but we sort only one of the two lists and compute the other on the fly. The preprocessing involves sorting s random numbers, requiring $O(s \log s)$ comparisons and $O(s)$ space. Sampled events are determined by walking through the sorted samples and the probability distribution, computing the cumulative sums along the way, requiring $O(n+s)$ computations. Sampled events are stored explicitly in space $O(s)$. Note that all memory accesses in this approach are contiguous (reads and writes). This returns an explicit sample list $\vec{e}$ of length s such that $e_1 \leq \cdots \leq e_\ell$.

Algorithm 4 Search via sample sorting (for $s < p$)

Given probability distribution $\vec{\rho} \in [0,1]^p$ and $s = \#$ samples
1: $r_\ell \leftarrow U(0,1)$ for all $\ell \in [s]$
2: Sort the vector $\vec{r}$ so that $r_1 \leq \cdots \leq r_\ell$
3: $k \leftarrow 1, \bar{\rho} \leftarrow \rho_k$
4: **for** $\ell = 1, \ldots, s$ **do**
5:     **while** $r_\ell > \bar{\rho}$ **do**
6:         $k \leftarrow k+1, \bar{\rho} \leftarrow \bar{\rho} + \rho_k$
7:     **end while**
8:     $e_\ell \leftarrow k$
9: **end for**

Thus, the cost of sampling and storing s events from a discrete distribution of size p is $O(s \log(\min\{s,p\}) + p)$ computations and $O(\min\{s,p\})$ space.

B. Diamond sampling with locality optimizations

The implementation of Algorithm 3 takes advantage of the specialized sorting mentioned above as well as locality, as we explain.
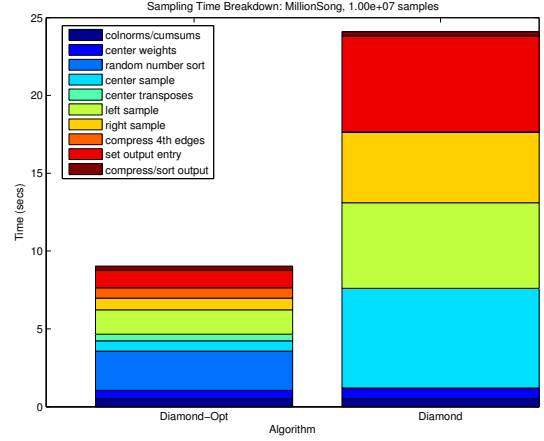

Fig. 4: Time breakdown for optimized and straightforward implementations of diamond sampling (Algorithm 3).

In the preprocessing, in anticipation of the sampling in Line 7, we compute a matrix $\hat{B}$ such that each row is a normalized cumulative sum, i.e., $\hat{b}_{kj} = \sum_{k' \leq k} b_{k'j}/\|b_{k*}\|_1$. We store the matrix $\hat{B}$ in compressed sparse row (CSR) format, so that the entries of $\hat{b}_{k*}$ are contiguous in memory. Similarly, for Line 8, we compute a matrix $\hat{A}$ such that each column is a normalized cumulative sum, i.e., $\hat{a}_{ki} = \sum_{i' \leq i} a_{ki'}/\|a_{*i}\|_1$. We store the matrix $\hat{A}$ in compressed sparse column (CSC) format, so that the entries of $\hat{a}_{i*}$ are contiguous in memory. Note that storage $\hat{A}$ in CSC format is equivalent to storage $\hat{A}^T$ in CSR format, so we need only one data structure.

We separate lines Lines 6 to 9 into four separate loops, first computing s pairs of the form (k, i), then s B-neighbors, etc.

For the samples in Line 6, we use the search via sample sorting in Algorithm 4 for choosing the samples from W since typically $\text{nnz}(W) = \text{nnz}(A) \gg s$. Because of the way that Algorithm 4 works, the pairs (k_ℓ, i_ℓ) for $\ell \in [s]$ are conveniently sorted according to k_ℓ.

The sorted values yield data locality for Line 7, where we use standard binary search to choose the values j_ℓ for $\ell \in [s]$.

We rearrange the s samples in $O(s)$ time so that they are ordered according to i_ℓ. Then we use standard binary search to choose the values k'_ℓ for $\ell \in [s]$ from Line 8.

Finally, we reorder the samples in $O(s)$ time so that they are sorted according to k'_ℓ, enabling efficient lookups for $b_{k'j}$ values in Line 9.

Fig. 4 shows a 2.7 times speed-up for our optimized implementation of Algorithm 3 versus a straightforward implementation. In particular, we note the drastic reduction in time for center, left, and right samples and setting the output entry (which involves searching for the existence of the 4th edge) in the optimized implementation. This is due to achieving better data locality (i.e., cache performance), and the overheads of the reorderings to attain this locality are amortized.

C. Exact computation (for comparison)

MAD corresponds to find the highest entries in a matrix-matrix product. General high-performance implementations

are available. In the dense case, the BLAS interface allows access to vendor-tuned libraries like Intel's Math Kernel Library [15] or NVIDIA's cuBLAS [34]. In the sparse case, matrix multiplication is available in CSparse [16], an efficient open-source library that is used by MATLAB for many sparse computations. The computational cost of matrix multiplication is $O(mnd)$ in the dense case (assuming the classical algorithm is used) and $O(\sum_k \deg_k^A \cdot \deg_k^B)$, i.e., the number of wedges in the tripartite graph, in the sparse case. The storage cost of library implementations of matrix multiplication, mn in the dense case and up to mn in the sparse case, is generally the limiting factor.

To adapt these high-performance libraries, we perform a series of matrix-vector products, $\vec{c_j} = A^T \vec{b_j}$ for $j \in [n]$, to compute the columns of C one at a time. We do not save the columns but instead use a priority queue to track the top-t entries. Because CSparse is open source, we were able to modify the code to minimize the memory footprint, achieving $O(\text{storage}(A) + \text{storage}(B) + t)$, with little loss in performance. In the dense case, we compute C in column blocks to size $n \times d$, computing and processing the output matrix in chunks using the dgemm interface to MKL, so that the memory footprint is $O(\text{storage}(A) + \text{storage}(B) + t)$.

VI. EXPERIMENTS

All experiments are run on an Intel Xeon E5-2650 "Ivy Bridge" 2.0 GHz machine with 32 GB of memory. Our codes are written in C/C++ with a mex-interface to MATLAB (Version 8.3.0.532). The codes are all single-threaded.

A. Datasets

We experiment on real-world datasets described below.

- *as-Skitter* $A^T A$: Skitter is an internet topology graph from the "as-Skitter" dataset from SNAP [35]. This yields a sparse binary symmetric $n \times n$ matrix A with $n = 1,696,415$ nodes and 11,095,298 nonzeros.
- *Movielens* $A^T B$: The Movielens-10M data set [31] comprises a sparse movie-user matrix, R, of size $m \times n$ with $m = 65,133$ movies and $n = 71,567$ users. Following Shrivastava and Li [9], who in turn followed [3], we compute the low-rank SVD of R using $d = 150$ components, so that $R \approx A^T B$ where $A \in \mathbb{R}^{d \times m}$ and $B \in \mathbb{R}^{d \times n}$ are dense real-valued matrices.
- *Live Journal* $A^T A$: LiveJournal is a free online community, and we use the "soc-LiveJournal1" dataset from SNAP [35]. The corresponding "friendship" sparse symmetric binary adjacency matrix A has dimension $n = 4,847,571$ and 68,993,773 nonzeros.
- *ASIC* $A^T A$: The ASIC dataset is a Xyce circuit simulation matrix; we use the "Sandia/ASIC_680k" matrix from the Florida matrix collection [36]. The $n \times n$ real-valued matrix A is nonsymmetric (though it is structurally symmetric) with dimension $n = 682,862$ and 2,638,997 nonzeros.
- *Amazon Kindle* $A^T B$: The Amazon product data consists of review and product data from Amazon [37], [38]. The

Kindle category data includes $m = 1,406,916$ reviewers and $n = 430,532$ books. The reviewer-book rating matrix A contains numeric scores from 1–5 for reviewed books and has a total of 3,205,546 entries. The book-book similarity matrix B contain numeric scores of 1–4 to indicate the relationship (i.e., 4 indicates the book have been purchased together by someone) with a total of 11,012,558 entries.

- *Million Song* $A^T A$: The Echo Nest Taste Profile Subset of the Million Song Dataset contains 48M user-song play counts from real users [10], [11], [12]. The resulting user-song matrix A has 1,019,318 users, 384,546 songs, and 48,373,586 user-song play counts.

B. Time and Accuracy Performance

We present time and accuracy results for six data sets in Figs. 5 and 6. In this study, we vary s as an axis, set $t' = s$, and plot results for $t \in \{1, 10, 100, 1000\}$. The top row plots the recall, i.e., the percentage of the top-t entries identified, versus the number of samples, s. (Not all samples close to form diamonds; see Table I.) The bottom row plots the wall-clock computation time versus the number of samples, including the time for exact computation as described in Section V-C. Because the budget t' does not depend on t (we set $t' = s$), the timing is the same for all runs. Table I contains some additional data about the sampling, including the size of the largest entry, the size of $\|W\|_1$, the ratio $\|W\|_1 / \max c_{ij}^2$ (which is proportional to the number of samples needed to recover the largest entry according to Theorem 4), and the closure rate of the three paths to form diamonds.

Dataset	max $|c_{ij}|$	$\|W\|_1$	est. samples	closure
as-Skitter	3.0e5	2.9e12	3e3	19%
Live Journal	3.0e3	1.5e12	1.6e5	13%
Movielens	1.1e0	2.8e10	2.3e8	100%
ASIC	2e12	9.6e19	2.4e-5	100%
Amazon Kindle	3.2e3	1.2e12	1.2e5	1.4%
Million Song	6.1e6	1.4e15	3.8e1	15%

TABLE I: Summary statistics for datasets. The column labeled "est. samples" reports the ratio $\|W\|_1 / \max c_{ij}^2$, the estimated number of samples required to find the top entry. The column labeled "closure" is the percentage of sampled three paths that correspond to a successful diamond sample.

For as-Skitter ($A^T A = A^2$ because input matrix A is symmetric; see Fig. 5), only 10^5 samples are required to capture all top 1000 entries in the output matrix, which requires 1.25 seconds (dominated by the preprocessing step). Exact computation, on the other hand, requires 160 seconds, which is 128 times slower. The top entry of this matrix has value 30,620, while the number of three paths $\|W\|_1$ is 2.9e12. The analysis in Section IV suggests that approximately 3000 samples are required to find the top entry (see Table I), and we identified the top entry after 1000 samples in this experiment. Likewise, the 1000th top entry in A^2 has value 4,239, the analysis suggests 16K samples, and only 10K were needed for this experiment. We find all top-1000 entries with only 10^6 samples, and only 19% of those samples turn into diamonds.
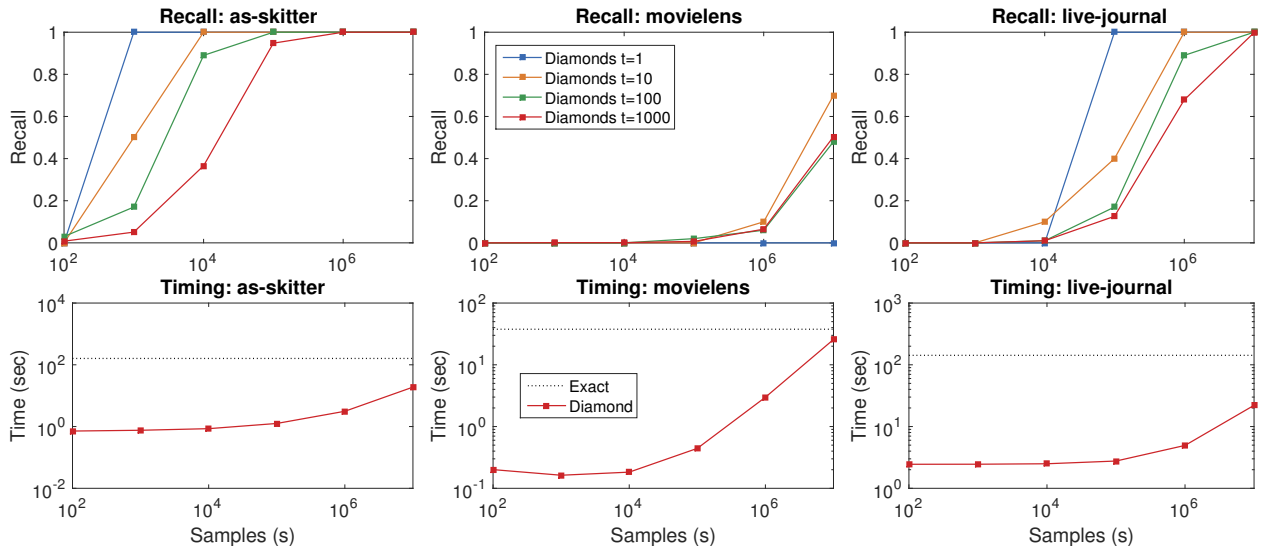
Fig. 5: Time and accuracy results for sampling approaches for datasets as-Skitter, Movielens, and Live Journal. The first row of plots presents the top-t scores over various numbers of samples, and the bottom row of plots shows the time in logarithmic scale.
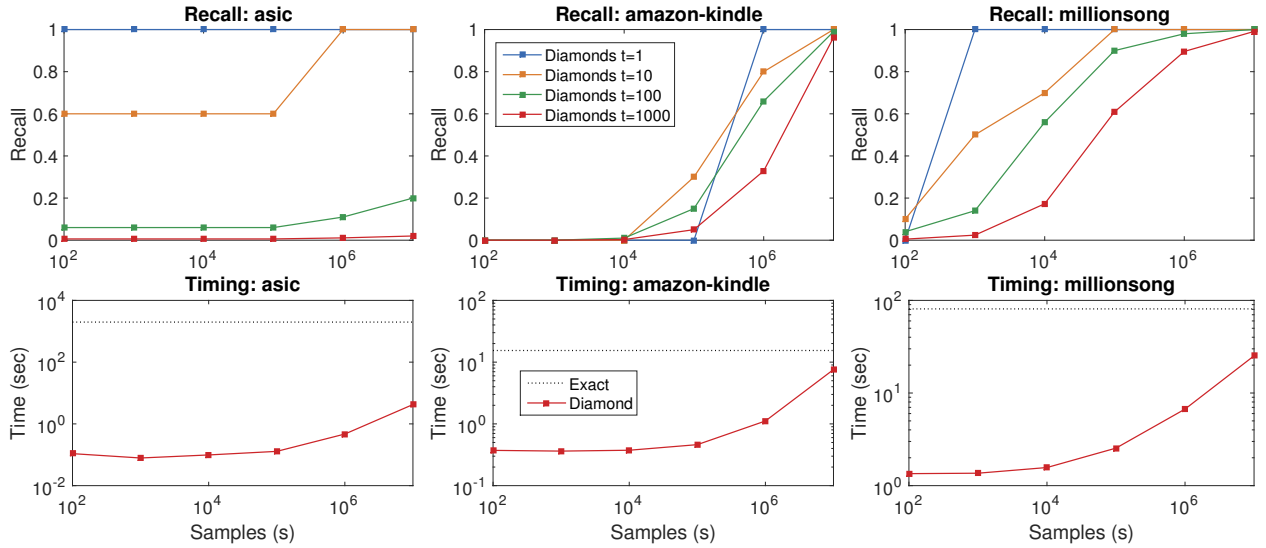

Fig. 6: Time and accuracy results for sampling approaches for datasets ASIC, Amazon Kindle, and Million Song. The first row of plots presents the recall scores over various numbers of samples, and the bottom row of plots shows the time in logarithmic scale.

MovieLens (dense $A^T B$; see Fig. 5) is the most difficult dataset because there is not much differentiation between the largest entries and smaller ones: the largest entry has magnitude 11.02 while the 1000th largest entry has magnitude 7.37. Also, the estimated number of samples just to get the top entry is 10^8; see Table I. Here, 10^7 samples is not sufficient and anything more requires more time than exact computation. The diamond closure rate is 100% because the matrices are dense. This is an example of a relatively small dataset where sampling is not effective; nevertheless, we still have impressive precision-recall results in Section VI-E.

In LiveJournal (sparse $A^T A$; see Fig. 5, we have $||W||_1 = 1.5 \times 10^{12}$ and the top entry is 2997, so we estimate needing $||W||/c_{ij}^2 \approx 10^5$ samples to find the largest entry (see Table I),

which is exactly when we find it. We find all top-1000 entries with 10^7 samples and 10X less time than exact computation.

The ASIC graph (sparse $A^T A$; see Fig. 6) comes from scientific computing. Here the largest few entries are very large compared to all others. For instance, the predicted number of samples is < 1 in Table I. So, we can identify the top-10 but struggle to identify the much smaller entries in the remainder of the top-1000 (10 million samples identifies only 703 distinct output entries). For the top-10, however, we have three orders of magnitude speed-up compared to exact computation.

We can find nearly the top-1000 for Amazon Kindle (sparse $A^T B$, see Fig. 6) using 10^7 samples, but the time is coming somewhat close to exact computation. This is a relatively small problem, and we expect that larger problems will have a more

significant benefit. The performance on the recommendation application in Fig. 7 yields good results.

We have 10X speed-up for the top-1000 entries for Million Song (sparse $A^T A$, see Fig. 6). We find the top entry after 1000 samples, which is a bit higher than the estimate in Table I of ≈ 100 samples.

C. Applications of MAD

SCENARIO 1 (FREE SAMPLES). A review site wants to encourage more reviews, so its goal is to select a limited number of reviewer-product pairs with the idea that the selected reviewer will be given a *free* item to review. We let A be a reviewer-by-product matrix and B is a product "also-bought" matrix. We then pick reviewer-product pairs, with the caveat that we should not give a reviewer something that they have already reviewed.

We use Amazon purchase data on reviews and product-product relationships [37], [38]. We focus on the Amazon Kindle subset, in which case we recommend e-books to be given to particular reviewers to solicit their reviews. Given the top recommendations for a free sample, we must check that the reviewer has not already reviewed the product; for this data set, about half of the top-t pairs correspond to new products for the particular reviewer. Fig. 7 shows an example top entry: it recommends a romance book to a user that has already reviewed many similar romance novels (three examples selected at random are shown).
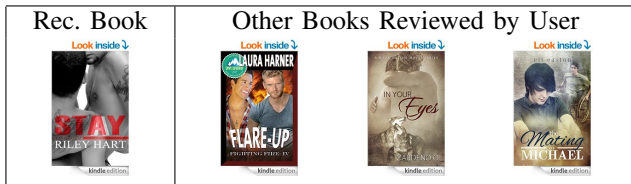

Rec. Book	Other Books Reviewed by User

Fig. 7: Example top pair from Amazon Kindle dataset: user ID 1317513 and the book entitled "Stay." The user has reviewed 649 other books, three random examples of which are shown.

SCENARIO 2 (2FOR1). A retailer wants to select, say, 100 pairs of products for a 2-for-the-price-of-1 promotion. If we assume each product has a dense or sparse representation in some feature space, this becomes a MAD search with $B = A$. In the case of the Million Song dataset, we let A denote a song-by-user matrix where entry (i, j) denotes the number of plays of song i by user j. We want to find pairs of distinct songs that have the highest number of common plays.

For this, we find the top-t pairs of similar songs in the Million Song dataset, based on being played by the same users. We calculate the top-t all-pairs dot products for columns of A as explained in Section III-B2. Additionally, we ignore the diagonal entries that pair songs with themselves. The top song pair using this metric is "Undo" by Björk and "Revelry" by Kings of Leon, which are both in the alternative genre.

SCENARIO 3 (LINK PREDICTION). We want to find members of a social network that should be connected but are not. These can be used as recommendations for new "friends."

We use the Live Journal data. The top entry in A^2 is not an edge in A; 6 out of top 10 are not; 55 out of top 100 are not; and 511 out of top 1000 are not. The top-10 new-connection suggestions have over 1800 common neighbors per pair.

D. Comparison to wedge sampling by Cohen-Lewis

The most similar related work is that of Cohen and Lewis [28], [8], which we refer to as wedge sampling. In this section, we compare diamond sampling to wedge sampling and present results for the Skitter dataset, which showed the most distinction between the methods. We generalized Cohen and Lewis' approach to t-MAD and implemented wedge sampling with similar optimizations to those described in Section V-B. In general, using diamonds requires fewer (three-path) samples than wedge samples to identify top entries in the output matrix. In our implementation, the preprocessing cost for diamonds is greater than for wedges, but the per-sample costs of each method are roughly the same.

In Fig. 8, we present top-t scores and times for wedge and diamond sampling on the Skitter dataset. In these experiments, we set the budget of dot products to be $t' = 1000 \cdot t$. For fewer than 10^5 samples, the diamond sampling has much better accuracy, but because the time is dominated by preprocessing, diamond sampling is also more expensive. For greater than 10^5 samples, the time is dominated by sampling and computing dot products, so the running times of diamond and wedge sampling approach are roughly the same. However, diamond sampling has identified all top entries by 10^5 samples, while wedge sampling needs 10^6 or 10^7 samples to identify all top entries, requiring an order of magnitude more time.
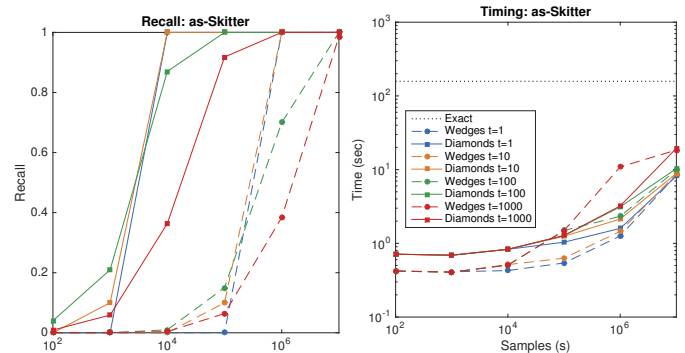

Fig. 8: Comparison of diamond sampling and wedge sampling.

E. Comparison to asymmetric LSH

We provide a comparison to some experiments in the paper by Shrivastava and Li [9] (additional details in [39]) for the Movielens-10M data set [31]. User j corresponds to column $\vec{b}_j$. For each user j, we want to find the top-10 movie recommendations. In other words, for each user, we want to solve the k-MIPS problem.

Precision-recall results over 2000 random users using asymmetric LSH and an increasing number of hash functions, $h \in \{ 64, 128, 256, 512 \}$, are reported in [9], [39]. The amount of storage increases with h. For comparison, we reproduce the curves reports in their figures, although we did not redo the experiments.

We also pick 2000 random users and apply our diamond sampling approach in Algorithm 3 repeatedly, using just a *single column* of B in each application. The A matrix is approximately 79MB in size. We need to keep one object that is the size of A and a few vectors of length m or s, for a total of less that 100MB extra storage. While it is hard to pin down the exact storage of LSH methods, it is on the order of one to two magnitudes more than the dataset. It is well-known that LSH is memory intensive (this is explicitly called out in the E2-LSH manual [40]).

We use an increasing number of samples, $s \in \{ 64, 128, 256, 512 \}$. We set the dot-product budget to be $t' = s$. Average precision-recall curves are shown in Fig. 9. It is difficult to compare the methods directly, so we cannot say that using 64 samples is comparable to using 64 hash functions. However, we can say that the storage per sample is much less than the storage per hash.
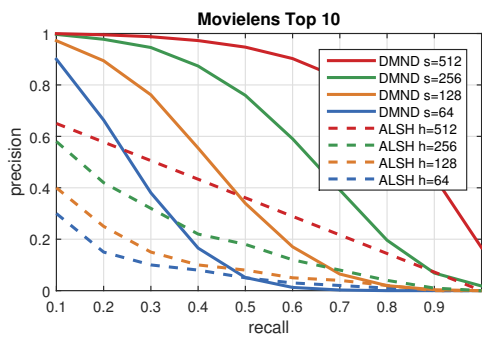

Fig. 9: Comparison of diamond sampling and asymmetric LSH.

References

[1] L. Adamic and E. Adar, "Friends and neighbors on the web," *Social Networks*, vol. 25, no. 3, pp. 211–230, 2003.

[2] D. Liben-Nowell and J. Kleinberg, "The link prediction problem for social networks," *J. American Soc. for Inf. Science and Tech.*, vol. 58, no. 7, pp. 1019–1031, 2007.

[3] P. Cremonesi, Y. Koren, and R. Turrin, "Performance of recommender algorithms on top-n recommendation tasks," *Proc. RecSys '10*, 2010. doi:10.1145/1864708.1864721

[4] G. Salton, J. Allan, and C. Buckley, "Approaches to passage retrieval in full text information systems," in *Proc. SIGIR '93* doi:10.1145/160688.160693. ISBN 0-89791-605-0 pp. 49–58.

[5] M. W. Berry, S. T. Dumais, and G. W. O'Brien, "Using linear algebra for intelligent information retrieval," *SIAM Review*, vol. 37, no. 4, pp. 573–595, 1995. doi:10.1137/1037127

[6] D. V. Kalashnikov, S. Mehrotra, and Z. Chen, "Exploiting relationships for domain-independent data cleaning," in *Proc. SDM'05*, Apr. 2005. doi:10.1137/1.9781611972757.24 pp. 262–273.

[7] F. Angiulli and C. Pizzuti, "An approximate algorithm for top-k closest pairs join query in large high dimensional data," *Data & Knowledge Engineering*, vol. 53, no. 3, pp. 263–281, Jun. 2005. doi:10.1016/j.datak.2004.08.003

[8] E. Cohen and D. D. Lewis, "Approximating matrix multiplication for pattern recognition tasks," *J. Algorithms*, vol. 30, no. 2, pp. 211–252, 1999. doi:10.1006/jagm.1998.0989

[9] A. Shrivastava and P. Li, "Asymmetric LSH (ALSH) for sublinear time maximum inner product search (MIPS)," in *NIPS 2014: Advances in Neural Information Processing Systems 27*, 2014, pp. 2321–2329.

[10] T. Bertin-Mahieux, D. P. W. Ellis, B. Whitman, and P. Lamere, "The million song dataset," in *Proc. ISMIR 2011*. University of Miami, 2011. http://hdl.handle.net/10022/AC:P:13628

[11] B. McFee, T. Bertin-Mahieux, D. P. Ellis, and G. R. Lanckriet, "The million song dataset challenge," in *WWW'12 Companion: Proc. 21st Intl. Conf. Companion on World Wide Web*, 2012. doi:10.1145/2187980.2188222 pp. 909–916.

[12] "The echo nest taste profile subset, the official user data collection for the million song dataset." http://labrosa.ee.columbia.edu/millionsong/tasteprofile

[13] F. G. Gustavson, "Two fast algorithms for sparse matrices: Multiplication and permuted transposition," *ACM T. Math. Soft.*, vol. 4, no. 3, pp. 250–269, Sep. 1978. doi:10.1145/355791.355796

[14] R. R. Amossen and R. Pagh, "Faster join-projects and sparse matrix multiplications," *ICDT '09* doi:10.1145/1514894.1514909 pp. 121–126.

[15] Intel, "Math kernel library reference manual," 2014, version 11.2. http://software.intel.com/en-us/articles/intel-math-kernel-library-documentation

[16] T. Davis, *Direct Methods for Sparse Linear Systems*. SIAM, 2006. http://epubs.siam.org/doi/abs/10.1137/1.9780898718881

[17] P. Drineas and R. Kannan, "Fast monte-carlo algorithms for approximate matrix multiplication," in *Proc. FoCS'01*, Oct. 2001. doi:10.1109/SFCS.2001.959921 pp. 452–459.

[18] P. Drineas, R. Kannan, and M. W. Mahoney, "Fast Monte Carlo algorithms for matrices I: Approximating matrix multiplication," *SIAM J. Computing*, vol. 36, no. 1, pp. 132–157, Jan. 2006. doi:10.1137/s0097539704442684

[19] P. Drineas and M. W. Mahoney, "On the Nyström method for approximating a gram matrix for improved kernel-based learning," *J. Mach. Learn. Res.*, vol. 6, pp. 2153–2175, Dec. 2005.

[20] T. Sarlós, "Improved approximation algorithms for large matrices via random projections," in *Proc. FOCS '06*, Oct. 2006. doi:10.1109/FOCS.2006.37 pp. 143–152.

[21] M.-A. Belabbas and P. Wolfe, "On sparse representations of linear operators and the approximation of matrix products," in *Proc. CISS 2008*, Mar. 2008. doi:10.1109/CISS.2008.4558532 pp. 258–263.

[22] A. Magen and A. Zouzias, "Low rank matrix-valued Chernoff bounds and approximate matrix multiplication," in *Proc. SODA '11*, 2011. doi:10.1137/1.9781611973082.109 pp. 1422–1436.

[23] R. Pagh, "Compressed matrix multiplication," *ACM Transactions on Computation Theory (TOCT)*, vol. 5, no. 3, pp. 1–17, Aug. 2013. doi:10.1145/2493252.2493254

[24] J. T. Holodnak and I. C. F. Ipsen, "Randomized approximation of the gram matrix: Exact computation and probabilistic bounds," *SIAM J. Matrix Analysis and Applications*, vol. 36, no. 1, pp. 110–137, 2015. doi:10.1137/130940116

[25] P. Indyk and R. Motwani, "Approximate nearest neighbors: Towards removing the curse of dimensionality," in *STOC 98*, 1998, pp. 604–613.

[26] A. Gionis, P. Indyk, and R. Motwani, "Similarity search in high dimensions via hashing," in *Proc. VLDB*, 1999, pp. 518–529.

[27] A. Andoni and P. Indyk, "Near-optimal hashing algorithms for approximate nearest neighbor in high dimensions," *Comm. ACM*, vol. 1, pp. 117–122, 2008.

[28] E. Cohen and D. D. Lewis, "Approximating matrix multiplication for pattern recognition tasks," in *SODA '97*, 1997, pp. 682–691. http://dl.acm.org/citation.cfm?id=314161.314415

[29] A. Campagna and R. Pagh, "Finding associations and computing similarity via biased pair sampling," *Knowledge and Information Systems*, vol. 31, no. 3, pp. 505–526, Jun. 2011. doi:10.1007/s10115-011-0428-y

[30] M. Jha, C. Seshadhri, and A. Pinar, "Path sampling: A fast and provable method for estimating 4-vertex subgraph counts," in *Proc. WWW'15*, 2015, in press.

[31] R. Davies, "Movielens 10m," GroupLens, Department of Computer Science and Engineering, University of Minnesota, Jan. 2009. http://files.grouplens.org/datasets/movielens/ml-10m-README.html

[32] D. Dubhashi and A. Panconesi, *Concentration of Measure for the Analysis of Randomised Algorithms*. Cambridge University Press, 2012.

[33] M. Vose, "A linear algorithm for generating random numbers with a given distribution," *IEEE T. Soft. Eng.*, vol. 17, no. 9, pp. 972–975, 1991. doi:10.1109/32.92917

[34] NVIDIA, "CUDA Toolkit Documentation: CUBLAS," available from http://docs.nvidia.com/cuda/cublas/index.html.

[35] J. Leskovec and A. Krevl, "SNAP Datasets: Stanford large network dataset collection," http://snap.stanford.edu/data, Jun. 2014.

[36] T. A. Davis and Y. Hu, "The university of florida sparse matrix collection," *ACM T. Math. Softw.*, vol. 38, no. 1, pp. 1:1–1:25, Dec. 2011. doi:10.1145/2049662.2049663.

[37] J. McAuley, C. Targett, J. Shi, and A. van den Hengel, "Image-based recommendations on styles and substitutes," in *Proc. SIGIR'15*, 2015. doi:10.1145/2766462.2767755.

[38] J. McAuley, "Amazon product data." http://jmcauley.ucsd.edu/data/amazon/

[39] A. Shrivastava and P. Li, "Asymmetric LSH (ALSH) for sublinear time maximum inner product search (MIPS)," arXiv:1405.5869, May 2014. http://arxiv.org/abs/1405.5869

[40] A. Andoni and P. Indyk, "E2-lsh manual," www.mit.edu/~andoni/LSH/manual.pdf.